An instrument to measure mechanical up-conversion phenomena in metals in the elastic regime

G. Vajente, E. A. Quintero, X. Ni, K. Arai, E. K. Gustafson, N. A. Robertson, E. J. Sanchez, J. R. Greer, and R. X. Adhikari

Citation: Review of Scientific Instruments **87**, 065107 (2016); doi: 10.1063/1.4953114
View online: https://doi.org/10.1063/1.4953114
View Table of Contents: http://aip.scitation.org/toc/rsi/87/6
Published by the American Institute of Physics

REVIEW OF SCIENTIFIC INSTRUMENTS **87**, 065107 (2016)

An instrument to measure mechanical up-conversion phenomena in metals in the elastic regime

G. Vajente,[1,a)] E. A. Quintero,[1] X. Ni,[2] K. Arai,[1] E. K. Gustafson,[1] N. A. Robertson,[1,3] E. J. Sanchez,[1] J. R. Greer,[2] and R. X. Adhikari[1]
[1]*LIGO Laboratory, California Institute of Technology, Pasadena, California 91125, USA*
[2]*Division of Engineering and Applied Sciences, California Institute of Technology, Pasadena, California 91125, USA*
[3]*SUPA, University of Glasgow, Glasgow G12 8QQ, United Kingdom*

(Received 24 March 2016; accepted 19 May 2016; published online 10 June 2016)

Crystalline materials, such as metals, are known to exhibit deviation from a simple linear relation between strain and stress when the latter exceeds the yield stress. In addition, it has been shown that metals respond to varying external stress in a discontinuous way in this regime, exhibiting discrete releases of energy. This *crackling noise* has been extensively studied both experimentally and theoretically when the metals are operating in the plastic regime. In our study, we focus on the behavior of metals in the elastic regime, where the stresses are well below the yield stress. We describe an instrument that aims to characterize non-linear mechanical noise in metals when stressed in the elastic regime. In macroscopic systems, this phenomenon is expected to manifest as a non-stationary noise modulated by external disturbances applied to the material, a form of mechanical up-conversion of noise. The main motivation for this work is for the case of maraging steel components (cantilevers and wires) in the suspension systems of terrestrial gravitational wave detectors. Such instruments are planned to reach very ambitious displacement sensitivities, and therefore mechanical noise in the cantilevers could prove to be a limiting factor for the detectors' final sensitivities, mainly due to non-linear up-conversion of low frequency residual seismic motion to the frequencies of interest for the gravitational wave observations. We describe here the experimental setup, with a target sensitivity of 10^{-15} m/$\sqrt{\text{Hz}}$ in the frequency range of 10–1000 Hz, a simple phenomenological model of the non-linear mechanical noise, and the analysis method that is inspired by this model. *Published by AIP Publishing.* [http://dx.doi.org/10.1063/1.4953114]

I. INTRODUCTION

Metallic materials are used in many mechanical systems, and we normally assume that they behave elastically, that is, the exhibited strain is proportional to the applied stress. However, it is well known that there are non-linear deviations that occur with loads that exceed the yield stress. Polycrystalline materials, which include most metal alloys, show more strain with incremental stress beyond the elastic regime, a behavior called plastic deformation, although the distinction between the elastic and plastic regime is not sharp.[13] Moreover, experimental observations at the microscopic scale have shown that, in this plastic regime, metal deformations are fundamentally not continuous, but instead happen through discrete releases of strain.[14] The resolved intermittent strain events, which exhibit scale-free statistics, are studied in a more general context as crackling noise.[20] In our study, we are interested in the possibility that similar non-linear phenomena could up-convert low frequency (below 1 Hz) excitations of the metals into high frequency (audio band) noise in their elastic regime.

It is important to emphasize here that, although some studies have already indicated deviations from a perfect elastic behavior in metals in relatively low stress conditions,[12] to the best of the authors' knowledge, there has been no direct measurement of mechanically up-converted noise, and all theoretical studies have been carried out when the material is in the plastic regime.

In our work, we are concerned with the possible influence of non-linear mechanical noise in the Advanced Laser Interferometer Gravitational-Wave Observatory (LIGO) detectors. The Advanced LIGO detectors are large-scale ground-based laser interferometers intended to observe gravitational waves.[3] To be successful, the LIGO detectors must reach an extreme displacement sensitivity in the audio frequency band. At the low frequency end of this band (10–20 Hz), the horizontal motion of the 40 kg fused silica mirrors, acting as test masses, must be only about 10^{-19} m/$\sqrt{\text{Hz}}$. Since the detector is located on the ground, it employs complex seismic isolation systems to reduce the contamination of the sensitivity by local seismic activity. The Advanced LIGO test mass suspension system,[5,18] shown schematically in Fig. 1, consists of a quadruple pendulum for horizontal isolation and incorporates three stages of 50 cm-long cantilever spring pairs, made of maraging steel[10] for vertical isolation. The suspension wires are also made of maraging steel, with the exception of the lowest wires, which are made of fused silica bonded to the mirror, to reduce thermal noise.[16] Any mechanical noise occurring within the cantilevers or in the wires will propagate to the test mass at some level. In particular, the lowest set of cantilever springs, which are installed in the second mass from the top (the

a)vajente@caltech.edu

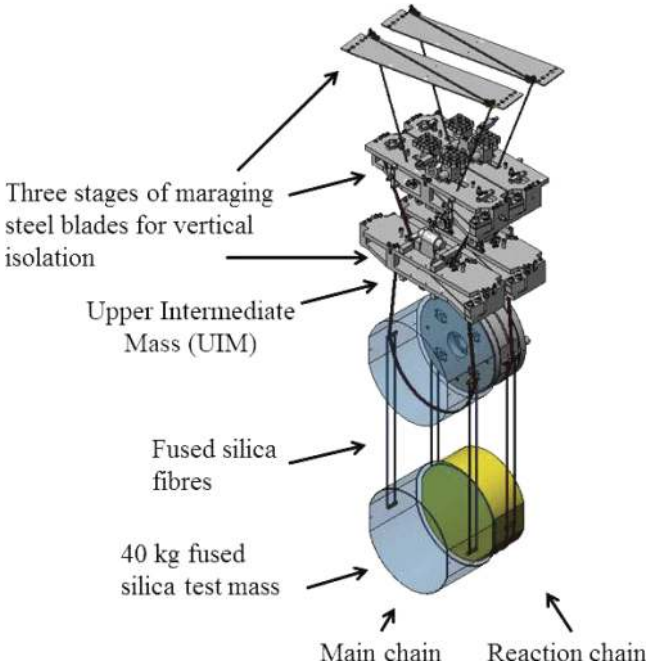

FIG. 1. The aLIGO test mass suspension system consists of a quadruple pendulum incorporating 3 stages of maraging steel cantilever springs. Drawing adapted from Ref. 5.

upper intermediate stage, or UIM), will couple most strongly to vertical displacement of the test mass, since there is less vertical isolation between them and the test mass than for those cantilevers that are higher up the chain. In turn, vertical motion of the test mass will couple to its horizontal displacement, which is the degree of freedom which is measured to detect gravitational waves, due to mechanical imbalances in the suspension system and, ultimately, to the Earth's curvature.[5] Thus, even if the impulsive strain events at the test mass are small, their combined influence can introduce background noise which could limit the interferometer sensitivity.

Metals can also exhibit creep noise.[8] Although the underlying micro-mechanics of mechanical up-conversion and creep may be related, creep has a event rate that decreases quickly after the initial stress, and experimental investigations have shown that the creep can be reduced with the use of maraging steel.[1,2,6,11] Our experiment however focuses on mechanical events that are continuously triggered by a time varying external perturbation, such as the Advanced LIGO suspension cantilevers which are subjected to by the local micro-seismic activity of the ground. In addition, since it is virtually impossible to distinguish between events happening in the cantilevers from those happening in the suspension wires or in the clamps, our system mimics as close as possible the Advanced LIGO configuration for cantilevers, wires, and clamps.

It is known that crackling noise occurs when metals are stressed in the plastic regime. In the Advanced LIGO suspension system, however, the cantilever and wires loads are solidly within the macroscopically elastic regime, specifically about 50% of the yield stress.[10] To the best of our knowledge, there has been no in-depth investigation for potential discrete, stochastic deviation from linear mechanical behavior in crystalline materials this far below the engineering yield stress. Nevertheless, we can borrow insights from the existing experiments and theories which have studied the problem in the plastic regime. First of all, micro-pillar compression tests have demonstrated the dependence of event size on the driving mode: under load-controlled mode large bursts are seen, while displacement-controlled mode leads to slipping events of smaller sizes.[17] It has also been shown that the distribution of the size of crackling events depends on the stress and stress rate,[15] being skewed toward smaller sizes for lower external stress and stress rate. These predictions have only been experimentally validated in the plastic regime, where burst sizes are large enough to exceed instrumental noises. Thus, the question of the existence of non-linear mechanical noise in the elastic regime remains open. Furthermore, the non-linear mechanical noise we are trying to characterize in the elastic regime — which we will hereafter refer to as *up-conversion noise* — can have intrinsically different physical origins from the crackling noise studied in the plastic regime.

Due to the novelty of this investigation and lack of a micro-mechanical model which predicts the exact form of the expected signals, our experiment follows a different approach with respect to what has been done previously. Instead of trying to detect individual slip events, we focus on the stochastic noise that would arise as a sum of a large number of small events. Such noise might have a non-stationary nature, with power depending on the external perturbation. In particular, given the performance of the Advanced LIGO seismic isolation system, we expect that residual low frequency motion of the suspension cantilevers could excite broadband mechanical noise, resulting in non-linear up-conversion and a broadband power spectrum of displacement noise, time-correlated with the driving force or force rate. Thus, we may expect an increased rate of larger events when the stress or stress rate of the cantilever is increased with respect to the equilibrium position.

II. MEASUREMENT METHOD

A direct measurement of the horizontal displacement noise introduced by up-conversion events in the Advanced LIGO suspension cantilevers would be impossible except with an apparatus which has the same displacement sensitivity as the Advanced LIGO interferometers.[3] However, any up-conversion noise at the level of the UIM cantilever springs will be attenuated by the additional vertical isolation provided by the lower suspension stages and by the relatively small coupling of vertical to horizontal test mass motion. For this reason, the sensitivity of our apparatus does not have to reach the Advanced LIGO level if we measure the vertical displacement of the cantilevers directly. A rough estimate of the sensitivity which is needed in our setup goes as follows. At 10 Hz, the Advanced LIGO design displacement noise is of the order of 4×10^{-19} m/$\sqrt{\text{Hz}}$.[3] Assuming a coupling of vertical to horizontal of the order of 10^{-4} due mainly to earth's curvature, this corresponds to a vertical displacement noise, at the test mass level, of 4×10^{-15} m/$\sqrt{\text{Hz}}$, without assuming any additional isolation between the test mass and the maraging cantilevers. This estimate has been confirmed using a model of the suspension system. Therefore we set a target sensitivity

for our system of 10^{-15} m/$\sqrt{\text{Hz}}$ at 10–20 Hz, which will be sufficient to probe up-conversion noise amplitudes relevant for Advanced LIGO.

However, as the magnitude of up-conversion noise is unknown and likely small, background noise sources will be a strong limiting factor in any measurement attempt. In view of this, an important component of our measurement strategy is to make a differential measurement of the motion of two cantilever springs that are arranged to make their response to background noise sources, such as seismic activity in the lab, as equal as possible. Since up-conversion noise occurs incoherently in each cantilever, a measurement of the cantilevers' differential displacement will be sensitive to up-conversion noise while rejecting any noise they have in common.

We choose to make this kind of differential measurement with a Michelson interferometer,[19] wherein a laser beam incident on a partially transmissive mirror is split into two beams which are retro-reflected by end mirrors mounted on masses suspended by the cantilever springs being tested for up-conversion noise, which we will refer to as the *test cantilevers* (see Figure 2). When these beams recombine at the beamsplitter, they will interfere constructively or destructively depending on the differential path length the beams traversed on their way to the end mirrors, providing a means of transduction of motion to optical power, which is then measured by a photodiode. Further details describing the optical signals present in the Michelson interferometer can be found in Section II A.

Furthermore, rather than trying to measure the up-conversion events due to ambient seismic motion, we can apply a controlled driving force, equal for both test cantilevers (*common mode*) to excite more up-conversion events. As will be explained in more detail in Section II C, this also allows us to enhance the apparatus' sensitivity by incorporating our knowledge of the drive and can provide insight into the micro-mechanical nature of the up-conversion events.

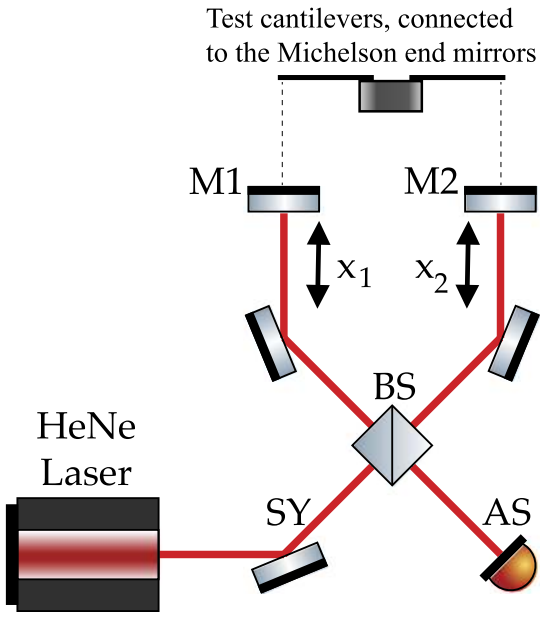

FIG. 2. Simplified schematic of the Michelson Interferometer layout employed. x_1 and x_2 represent the motion of mirrors 1 and 2, which are suspended from test cantilevers 1 and 2 (not shown). "SY" and "AS" refer to the "symmetric" and "anti-symmetric" ports, respectively.

A. Utility of the Michelson interferometer

A schematically representative diagram of the interferometer design is shown in Fig. 2. The quantities x_1 and x_2 represent the vertical displacement of the end mirrors, M1 and M2, from the equilibrium position of the cantilever springs they are suspended from. For the sake of convenience, we will assume that the optical path lengths between the beamsplitter and each end mirror are equal; this requirement will be relaxed in Section IV A. As a first step, we consider the optical signal present at the photodiode at the anti-symmetric port of the interferometer, labeled "AS" in Fig. 2.

We will consider the laser light's field amplitude incident on the beamsplitter to be of the form

$$E_{\text{in}} = E_0 e^{i\omega t},$$

where ω denotes the frequency of the laser light source, related to the wavelength $\lambda = \frac{2\pi c}{\omega}$ and to the wave number $k = \frac{2\pi}{\lambda}$. Then, the field exiting the beamsplitter at the AS port will be the superposition of the fields which independently traversed the two arms of the interferometer,

$$E_{\text{AS}} = E_1 - E_2, \quad \text{where} \tag{1}$$
$$E_{\text{i}} = \tfrac{1}{2} E_{\text{in}} e^{2ik(L+x_{\text{i}})}, \tag{2}$$

where L is the distance from the beamsplitter to the equilibrium point of each end mirror and, in the second equation, $i = 1, 2$ refer to the field propagating in the two interferometer arms. The minus sign in Eq. (1) is due to the fact that the field returning from mirror 2 reflects off of the back surface of the beamsplitter, and thus experiences a π phase shift relative to the light which reflected off of mirror 1 and the front surface of the beamsplitter.

Thus, the field amplitude and intensity at the AS port are given by

$$E_{\text{AS}} = \tfrac{1}{2} E_{\text{in}} e^{ik2L} (e^{ikx_1} - e^{ikx_2}), \tag{3}$$
$$I_{\text{AS}} = E^*_{\text{AS}} E_{\text{AS}} = \tfrac{1}{2} E^2_{\text{in}} [1 - \cos(k(x_1 - x_2))]. \tag{4}$$

Eq. (4) shows the optical power measured by a photodiode at the AS port, which is a function of the positions of the two end mirrors. Thus, the Michelson interferometer naturally provides an optical signal that is only sensitive to differential displacements of the two test cantilevers, providing, ideally, an infinite rejection of common mode motion.

However, the linear range of the signal is limited by the wavelength of the light used, as can be seen by the sinusoidal functions of the displacement. So, to ensure linear readout, active feedback is used to keep the interferometer at the proper operating point.[7] Specifically, we employ a feedback loop that stabilizes the differential displacement by applying differential force to the tip of the test cantilevers that is continuously tuned to maintain constant power incident on the photodiode. This does not reduce the information present in the system, as one can reconstruct the linear open-loop behavior of the system by appropriately combining the feedback control and error signals.

A potential flaw with this optical readout scheme is the inability to distinguish fluctuations in the laser source intensity from real displacement fluctuations; the signal described in

Eq. (4) is linearly proportional to the input laser power. The solution to this issue is to read out both interferometer outputs: the symmetric port, as described above, in addition to the anti-symmetric port, "SY." By injecting the input beam at an angle, one can cleanly separate both output beams (see Fig. 6). The signal at the symmetric port can be easily written down by conservation of energy from Eq. (4),

$$I_{\mathrm{SY}} = \tfrac{1}{2} E_{\mathrm{in}}^2 \left(1 + \cos\left(k\left(x_1 - x_2\right)\right)\right). \tag{5}$$

We can now construct a signal that suppresses the linear coupling of intensity to position readout by subtracting the two signals, either with analog electronics or within a digital control and data acquisition system,

$$\begin{aligned} x_e &= I_{\mathrm{SY}} - I_{\mathrm{AS}} \\ &= E_{\mathrm{in}}^2 \cos\left(k\left(x_1 - x_2\right)\right). \end{aligned} \tag{6}$$

With the aid of the feedback control loop, we actuate on the differential mirror positions, which constrains this signal to remain close to zero, which in turn eliminates the direct linear coupling of laser intensity noise to our displacement signal. This interference condition is often called the *half-fringe*, meaning that the power at the two detectors is equal: half of the input power.

An ideal Michelson interferometer is insensitive to laser frequency noise. However, any mismatch, ΔL, in the length of the two Michelson arms will result in a coupling of laser frequency noise to the output port powers. Indeed, starting from Eq. (1) and considering that a variation in the laser frequency corresponds to a variation of k, it is easy to show that a change in the laser frequency $\delta\omega$ will introduce a power variation equivalent to a differential displacement of the end mirror δx, given by

$$\delta x = \frac{\Delta L}{\omega} \delta\omega. \tag{7}$$

Therefore frequency noise of the laser can be ignored if the length of the two Michelson arms is equalized to within a good accuracy. As discussed below, the safest approach is to implement a way to remotely equalize the length of the two arms.

Finally, although a Michelson interferometer is first order insensitive to translation and rotation of the input beam, any misalignment of the end mirrors translates in a change of the interference of the beams at the output ports, resulting in a reduction of the optical gain. If the vertical motion of the two test cantilevers translates to a differential angular motion of the end mirrors, an additional up-conversion mechanism will be present that can mimic the one we are looking for, as discussed below. For this reason, it is important to install the two blades in an anti-parallel configuration and decouple efficiently the mirror angular motion from the cantilever. As discussed below, this is done by suspending the mirrors with thin wires.

B. Up-conversion noise model

In the absent of a detailed micro-mechanical model, we can instead use a simple phenomenological model informed by analogous physical processes, such as Barkhausen noise in magnetized materials,[22] to design our analysis method. Specifically, we model the effect of up-conversion events in a cantilever spring as a stochastic displacement noise with unknown spectral properties, but with a magnitude determined by the applied force and/or its derivative. Since this stochastic noise is the result of the sum of a large number of microscopic events, its statistical properties depend on the rate and size distribution of such events. We expect those properties to depend both on material properties and on the local stress or stress rate in each parts of the cantilever. We focus our attention on the case of a cantilever which is subject to a possibly large static load and a time varying external perturbation, typically induced by an external low frequency force. The static load might induce some creep in the metal, but this phenomenon is well known and its magnitude reduces over time.[8]

Thus, we consider a cantilever subject to a time dependent force $F(t)$, with a characteristic frequency below the macroscopical resonance of the cantilever. In this case, the local microscopic stress varies over time following the external drive. Thus, we write the up-conversion noise contribution to the displacement as

$$x_{\mathrm{up-conversion}}(t) = \chi\left[F(t)\right] \delta x_{\mathrm{f}}(t) + \theta\left[\dot{F}(t)\right] \delta x_{\mathrm{j}}(t), \tag{8}$$

where δx_{f} and δx_{j} are stochastic processes representing the force- and jerk-dependent up-conversion, and χ and θ are the functional forms of the noise dependence on the applied force and its derivative. They reflect the intensity of up-conversion noise in the specific cantilever, and they may be a function of drive frequency and amplitude, in addition to the static load, cantilever geometry, and material properties.

An important observation can be made at this point. The δx_f and δx_j terms will in general have nonzero spectral content at the frequencies in the LIGO detection band (10–5000 Hz). On the other hand, the typical force $F(t)$ on the cantilevers is due to the residual coupling of ground motion through the suspension system, which acts as a steep low pass filter with corner frequency of the order of a few hertz. Therefore, while $F(t)$ has very low amplitude at higher frequencies, the large amplitudes at low frequency can excite up-conversion events, generating noise in the audio band. Thus, it is important to measure the level of non-linear up-conversions from large static strains and low-frequency motions to noise in the audio band, where Advanced LIGO is most sensitive to gravitational waves.

C. Demodulation analysis

In order to excite up-conversion events, we introduce a low frequency, common mode excitation in the two test cantilevers through the application of a force in the form of $F(t) = F_0 \sin(\omega_d t)$, that is much larger than the residual seismic motion.

To mimic the conditions in the Advanced LIGO suspension, this time-varying force is small when compared to the static load applied on the cantilever; in our test setup, for example, the static load is of the order of 20 N, while the time varying common mode drive is of the order of few mN. Therefore we can expand, by a Taylor series, the two functions

χ and θ around the point corresponding to the static load. With this assumption, the individual cantilever displacements are given as

$$x_i(t) = \frac{F_0 \sin(\omega_d t)}{k} + \frac{\alpha}{\sqrt{2}} F_0 \sin(\omega_d t)\delta x_{\mathrm{f},i}(t) + \frac{\beta}{\sqrt{2}} F_0 \omega_d \cos(\omega_d t)\, \delta x_{\mathrm{j},i}(t), \quad (9)$$

where k is the cantilever elastic spring constant and the factors of $\sqrt{2}$ have been introduced to simplify later equations. In the differential displacement signal, the elastic responses of the cantilevers will cancel out, leaving the incoherent sums of the up-conversion noise terms. In practice, this will not be the only signal present; there will be many background noise sources. It can occur that the displacement due to up-conversion noise is smaller than the background noise in a given frequency band, and thus will not be directly observed. However, many background noise sources — such as shot noise on the photodetectors, intensity noise of the laser, and seismic noise that couples through mechanical asymmetries — can be assumed to be quasi-stationary and have no dependence on the common mode drive. Instead, it can be seen that the up-conversion signal written above varies in a known way with the applied drive; using this additional information, we can potentially extract this signal from underneath stationary background noise, as will now be explained.

We condense the total differential displacement due to up-conversion noise and some stationary background noise $n(t)$, combining the incoherent sums of up-conversion noise in each cantilever into a single term,

$$\Delta x(t) = n(t) + \alpha F_0 \sin(\omega_d t)\, \delta x_{\mathrm{f}} + \beta F_0 \omega_d \cos(\omega_d t)\, \delta x_{\mathrm{j}}. \quad (10)$$

An example of how the δx_{j} term manifests itself is shown in Fig. 3.

We now want to take advantage of the periodicity and phase of the envelope of the up-conversion noise processes and analyze the instantaneous power of the displacement time series, i.e., its square. Simple algebraic computations yield

$$\begin{aligned}\Delta x^2(t) = {} & 2n(t)F_0\left[\alpha \sin(\omega_d t)\delta x_{\mathrm{f}} + \beta\omega_d \cos(\omega_d t)\delta x_{\mathrm{j}}\right] \\ & + n(t)^2 + \frac{F_0}{2}\left[\alpha^2 \delta x_{\mathrm{f}}^2 + \beta^2 \omega_d^2 \delta x_j^2\right] \\ & + \cos(2\omega_d t)\frac{F_0}{2}\left[-\alpha^2 \delta x_{\mathrm{f}}^2 + \beta^2 \omega_d^2 \delta x_{\mathrm{j}}^2\right] \\ & + \sin(2\omega_d t) F_0 \alpha\beta \delta x_{\mathrm{f}} \delta x_{\mathrm{j}}. \end{aligned} \quad (11)$$

We can average the above quantity over a period longer than the typical time scale of the random processes, and slower than the external drive sinusoid. Assuming that $n(t), \delta x_{\mathrm{f}}(t)$, $\delta x_{\mathrm{j}}(t)$ are independent zero-mean random noise processes, the first and last lines will have expectation values of zero, while the second line will have some constant expectation value. In contrast, the $\cos(2\omega_d t)$ term provides a time varying component at a known frequency, with a known phase with respect to the driving force. Writing the Fourier transform of the power signal as $\tilde{P}(\omega)$, we can take the expectation value at $2\omega_d$, or *demodulate* the drive-modulated signal, to see the power fluctuations due to up-conversion events,

$$\langle \tilde{P}(2\omega_d) \rangle = \frac{F_0}{4}\left(-\alpha^2 \delta x_{\mathrm{f}}^2 + \beta^2 \omega_d^2 \delta x_{\mathrm{j}}^2\right). \quad (12)$$

In addition, by integrating for many cycles, the determination of the up-conversion noise amplitude of Eq. (12) improves proportionally to the square root of integration time. Thus, it is possible to increase the measurement time to find up-conversion noise power varying with the modeled phase and frequency, even below the background noise.

Furthermore, the common drive can be switched off, which should result in a demodulation result of zero, on average. Thus, we can sample the magnitude of the demodulation amplitude in two different states: with the drive on and up-conversion noise present, and with the drive off and no up-conversion noise present. We expect to observe different means in the underlying distributions, as shown in Fig. 4.

Thus, the analysis of confidence and uncertainty in our measured results reduces to the standard analysis of whether

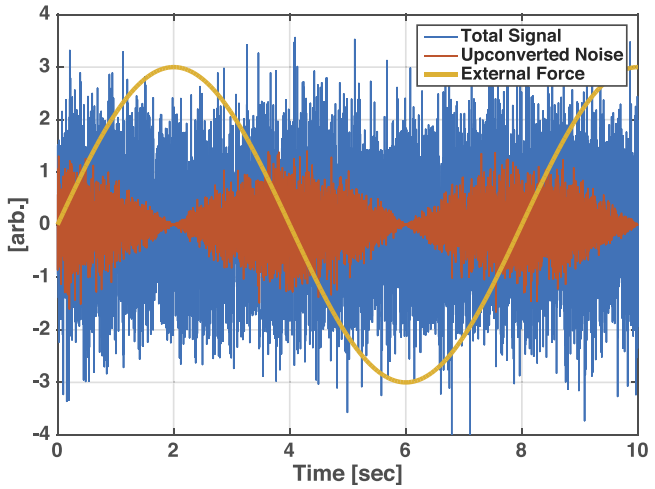

FIG. 3. A qualitative illustration of the signal described in Eq. (10), with simulated data. In this case we have assumed that the up-conversion noise is proportional to the derivative of the external drive, therefore the up-conversion noise power is larger when the sinusoidal excitation crosses zero.

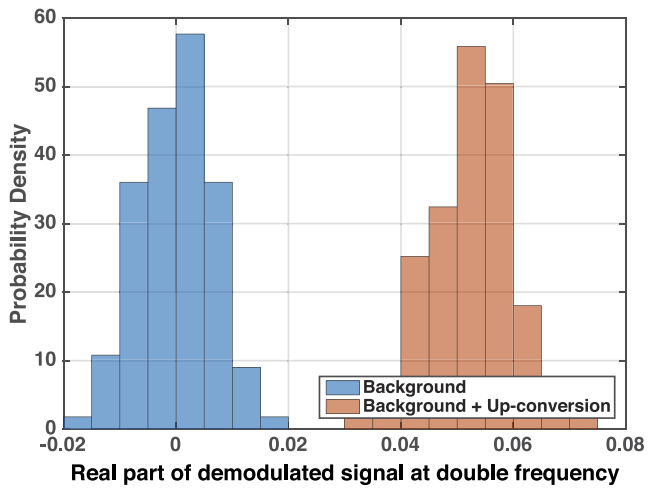

FIG. 4. Result of the demodulation described in Eq. (12) of 30 min of simulated data with background and up-conversion noise levels as in Fig. 3. The distributions are clearly separated, showing a strong up-conversion noise signature.

the two sets of data are unlikely to arise from the same underlying probability distribution. Then, appropriate statistical methods, such as the Student's t-test, can be used to determine if a statistically significant difference in the means of the two sets of results is present or to derive confidence intervals on the upper bound of the difference in the means consistent with our observations. This manner of statistical validation would provide a strong argument for the observation of up-conversion noise.

In practice, the functional dependence of the up-conversion noise on the applied force is unlikely to take the simple linear form we used above. The model can be generalized by writing out more terms in the Taylor expansion of the χ and θ functions and working out the corresponding periodic fluctuations expected in the displacement power time series. Thus, by examining different harmonics of the drive frequency, we can potentially infer the form of χ and/or θ and the micromechanical phenomena they arise from. Without going into the details of those computations, it suffices to say that the analysis will be carried out looking at various frequency components of the up-conversion noise amplitude: at the drive frequency, the second and the fourth harmonics. Additionally, we will allow for modulation both in-phase and in quadrature with respect to the drive.

Finally, while demodulation techniques such as we have described here are useful for discriminating periodic signals from stationary background, there are additional systematic effects from background noise that are also modulated by the common-mode drive and thereby not easily distinguishable from true up-conversion noise. Examples include Barkhausen noise of the magnets used in the electromagnetic actuators driving the test cantilevers or modulation of the power detected at the photodiode induced by misalignments of the end mirrors due to the common-mode drive. These effects are ideally minimized via careful experimental design and construction, and their contributions to the demodulated signals quantified and accounted for. Section IV will discuss these effects in more detail.

III. THE INITIAL PROTOTYPE OF THE MEASUREMENT SYSTEM

An initial prototype for this experiment consisted of a Michelson interferometer, with end mirrors attached to the bottom of load masses clamped to the tips of small test cantilevers that were used in Advanced LIGO prototype suspensions. The cantilevers were clamped to a single tall post and in turn attached to an optical board, where the horizontal Michelson interferometer was mounted. The need to measure vertical motion of the test cantilevers while the interferometer was arranged horizontally introduced additional complexity to the system and reduced its overall rigidity.

The load was rigidly clamped to the tip of the test cantilever. This approach had several drawbacks. First of all, any vertical motion of the cantilever tip coupled directly to a tilt of the load mass and of the Michelson end mirror. In turn, this misalignment of the Michelson was a limiting factor for the maximum amplitude of the common mode displacement we could exert. Second, this rigid clamp also coupled all of the cantilever transverse and torsional modes to angular motion of the mirror, introducing additional complexity to the actuation and control of the system.

The apparatus was housed in a vacuum chamber to mitigate acoustic noise and mounted on a stack of two plates standing on rubber springs to reduce seismic noise. Outside of the chamber, a free-running polarized HeNe laser was coupled into a single mode, polarization maintaining, fiber optic cable, which then was fed through to the interior of the chamber.

While the prototype reached a sensitivity on the order of 10^{-15} m/$\sqrt{\text{Hz}}$ above 400 Hz, the sensitivity at lower frequencies was greatly limited by poor seismic isolation, which, in turn, was limited by the available space inside of the available vacuum chamber.

Mitigating these issues became the main consideration when designing the second iteration of the experiment. Specifically, we decided to suspend the cantilevers' load masses with steel wires to reduce the coupling of higher order vibrational modes of the cantilevers and to construct a two stage pendulum seismic isolation system to attempt to reach a sensitivity of 10^{-15} m/$\sqrt{\text{Hz}}$ at 10 Hz. This figure is motivated by the sensitivity at which a null result would suggest that up-conversion noise would not be a limiting noise source for Advanced LIGO.

Concretely, with the first iteration of the apparatus, we set an upper limit on the possible up-conversion noise when the cantilevers were subjected to a 1 μm common mode displacement of 3×10^{-15} m/$\sqrt{\text{Hz}}$ in the band from 450 to 500 Hz.[21] However, without a clear observation or verified physical model, the frequency dependence of the noise is unknown — though perhaps reasonably lying between f^{-3} and f^{-1} — making it difficult to extrapolate this upper limit to frequencies relevant for Advanced LIGO. Depending on the noise model used, the extrapolated noise at 10 Hz varies dramatically. From our prototype's upper limit, we computed an upper limit of the amplitude spectral density of up-conversion noise in the Advanced LIGO upper intermediate mass (UIM, see Fig. 1) cantilever tips propagating to the gravitational wave strain readout anywhere from 2.4×10^{-21} m/$\sqrt{\text{Hz}}$ to 4×10^{-18} m/$\sqrt{\text{Hz}}$, depending on the spectral profile of up-conversion noise, where the Advanced LIGO design sensitivity at 10 Hz is approximately 8×10^{-19} m/$\sqrt{\text{Hz}}$.[21] Therefore the results obtained with the prototype were not good enough to rule out up-conversion noise as an important factor in Advanced LIGO's sensitivity.

IV. THE IMPROVED MEASUREMENT SYSTEM

The limitations found during the operation of the first measurement system prompted us to design an upgraded, more sensitive measurement system. The scientific goal of the new system is to reach a displacement sensitivity of the differential motion of the tip of the two test cantilevers of the order of 10^{-15} m/$\sqrt{\text{Hz}}$, at frequencies of 10 ~ 20 Hz and above, thus improving by many orders of magnitude our capability to detect up-conversion noise in the low frequency region.

This section describes the main features of the new system: passive suspension of the optical board to achieve better

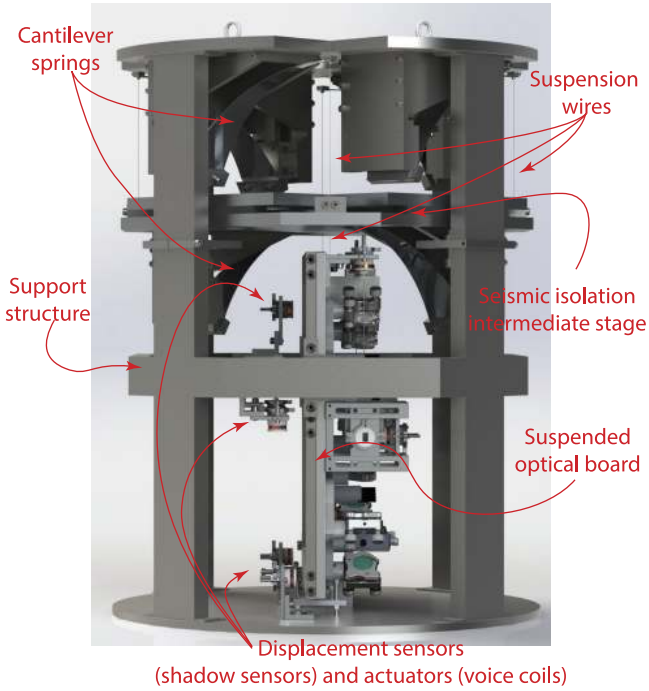

FIG. 5. Three dimensional rendering of the new measurement apparatus (Sec. IV), showing the suspended optical breadboard (Sec. IV A), the seismic isolation system (Sec. IV C) and the support structure.

isolation from seismic ground motion; use of a near infrared Nd:YAG source to reduce the laser technical noises; and an improved design of the test cantilever load, clamp, and displacement readout.

Fig. 5 shows a three dimensional rendering of the new instrument. The optical board that holds the Michelson interferometer hangs vertically inside the support structure. The breadboard is suspended by two stages of vertical and horizontal isolation. Its motion is sensed and controlled using six integrated shadow sensor and voice coil actuators. More details on the seismic isolation system are given in Sec. IV C. The entire system is housed inside a vacuum chamber, to reduce contamination of the optics, noise due to air fluctuations, and acoustic disturbances.

A. Optical system

Fig. 6 shows a schematic of the optical layout. As described above, the readout system is a Michelson interferometer. The two end mirrors of the Michelson interferometer must be horizontal, since they should measure the vertical displacement of the test cantilevers. For this reason, the entire optical system is mounted on a vertical 40×45 cm board. This allows us to have a much more rigid structure, compared to the first prototype system. The light source is a 1064 nm wavelength Nd:YAG NPRO (Non-Planar Ring Oscillator) laser, which delivers a typical power of 10–20 mW into the interferometer. This power level is enough to reach a shot noise limited sensitivity better than 10^{-15} m/$\sqrt{\text{Hz}}$ over the entire band of interest. The laser is not actively stabilized in either intensity or frequency at this time. The laser beam enters through a viewport (not shown) on the bottom left side of the board and is steered into the beamsplitter by two adjustable mirrors. The two arms of the Michelson interferometer are folded in such a way that the beam is almost vertically incident on the two interferometer end mirrors. They are mounted on two 2.2 kg blocks that are suspended with wires from the two test cantilevers. Lateral motion of the two blocks is also sensed and mitigated with the same kind of integrated sensors-actuators that are used for the main optical board. Both test cantilevers are clamped to the same support visible in the top center of the board. On the two cantilever tips, there are two additional displacement sensors and actuators (not shown in the figure) that are used both to maintain the correct half-fringe operating point of the interferometer and to apply the common mode low frequency drive that would excite up-conversion noise. The symmetric and anti-symmetric beams recombining at the beamsplitter are picked up by two additional steering mirrors and sent to two photodiodes.

The typical free running frequency noise of an NPRO system like the one we used in Ref. 9 is on the order of 100 Hz/$\sqrt{\text{Hz}}$ at 100 Hz and decreases as $1/f$. The coupling depends on the Michelson arm length difference, as discussed above. So, to reach our design sensitivity at 10 Hz, the length difference of the arms must be smaller than 0.3 mm. This level of accuracy is not easily obtainable in the installation phase of the optical system. For this reason, one of the two folding mirrors in the interferometer (Fig. 6) is mounted on a linear motorized translation stage. It is then possible to add an external perturbation on the laser frequency and directly measure the coupling to the Michelson displacement signal. This can be converted into a length difference, with Eq. (7), that can be corrected using the translation stage. This procedure allows us to achieve the needed length balancing. The other folding mirror is mounted on a motorized angular stage, to allow us to fine tune the interferometer alignment in vacuum.

B. Improved test cantilever assembly

The two test cantilevers are pre-curved in such a way that when they are loaded at about 50% of their yield stress (corresponding to 2.2 kg in our case), they are flat. The transverse profile of the cantilever is triangular: in this way the initial curvature is constant along the entire length of the cantilever, and, moreover, the static stress due to the load is constant along the cantilever, except of course close to the clamp, where there is some localized increase of stress.

The load mass is attached to the cantilever through a single steel wire. In this way we obtain a very high decoupling of any torsional and angular motion of the cantilever tip from angular motions of the Michelson mirror, which is rigidly attached to the bottom of the load mass. Indeed the load mass is isolated from lateral motion of the cantilever tip by a pendulum, and from any angular motion by the stiffness of the wire itself, which can be made very small. Moreover, the wire is clamped to the cantilever with two small steel blocks, held together with bolts. This is a scaled down version of the clamp used in the Advanced LIGO system, and it provides a clean solution that avoids friction and additional stress. Additionally, it serves the purpose of making the test system as similar as possible to the system used in the gravitational wave detectors.

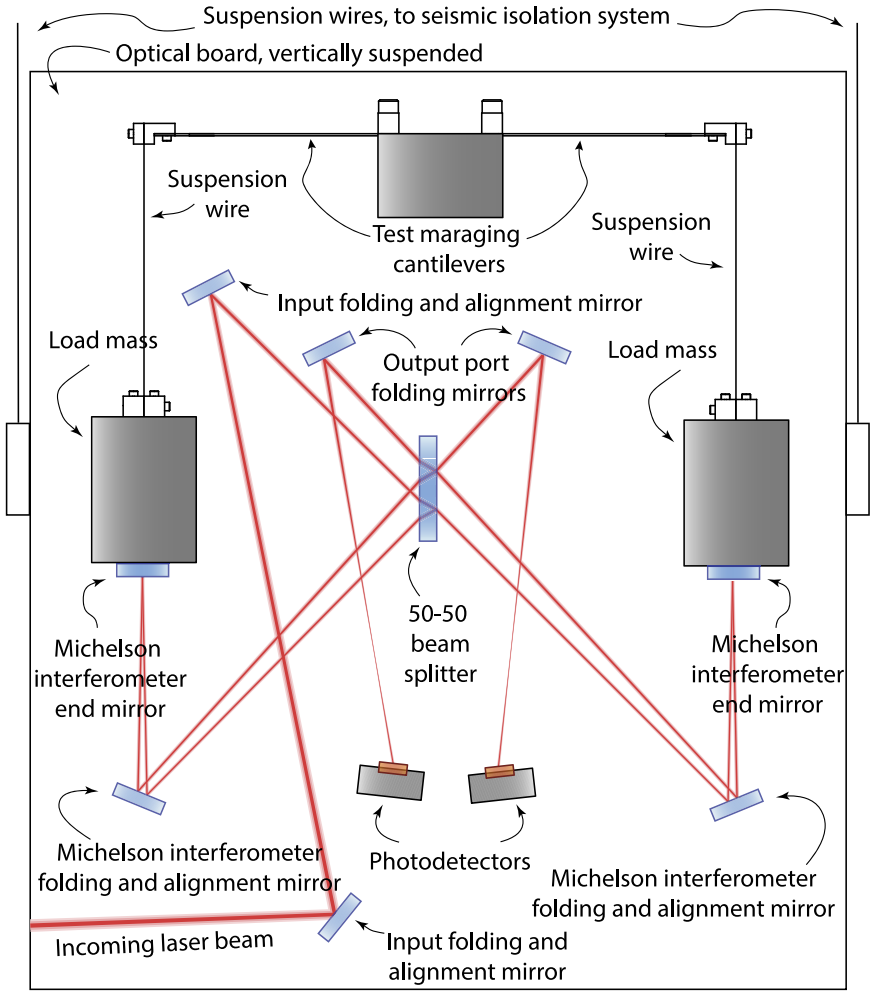

FIG. 6. Simplified optical scheme of the Michelson interferometer. Only the main beams and optical components are shown: reflections from the secondary surfaces and beam dumps are not drawn for simplicity. Also, actuators and displacement sensors have been removed.

C. Seismic isolation

The dominant limitation to the sensitivity of the first version of the measurement system was seismic noise at frequencies below a few hundred Hz. Indeed, the ground motion in a typical urban ground location can be many orders of magnitude larger than our target sensitivity. The measured motion of an optical table in our lab showed a displacement noise of the order 10^{-8} m/$\sqrt{\text{Hz}}$ at 10 Hz, decreasing with frequency roughly like f^{-3}. The most important degree of freedom in our system is the vertical one, since this corresponds to the direction of the Michelson interferometer measurement. Ideally, if the optical system was infinitely rigid and the two test cantilevers were exactly equal, any vertical motion of the optical breadboard would result in a common mode variation of the interferometer arm lengths. Thus, since a Michelson interferometer has virtually infinite common mode rejection, it should not be affected by seismic motion of the ground. However, there is a limit to the level the two cantilevers can be made equal: in particular, differences in the material, machining, and clamping can result in a mismatch of the resonant frequency and of the distance from the clamp to the wire suspension point. A trade-off is necessary between the requirements on the cantilever equality and the performance of the seismic isolation system: a worse matching of resonant frequency or distance would require increased performance on the suspension system. It can be shown using a simple elastic model of the two cantilevers that the residual coupling of common vertical motion x_{comm} to differential displacement x_{diff} of the two cantilever tips is given by

$$\frac{x_{\text{diff}}}{x_{\text{comm}}} \sim \left(\frac{f_0}{f}\right)^2 \left[2\frac{\delta f_0}{f_0} + \frac{\delta L}{L}\right], \tag{13}$$

where f is the measurement frequency, f_0 is the cantilever mean resonant frequency, δf_0 is the difference between the two resonant frequencies, L is the mean of the cantilever's length from the clamp to the wire attachment point, and δL is the length mismatch. The two expressions above are correct for frequencies larger than f_0 (about 2 Hz) and smaller than the first higher order resonance of the loaded cantilever (about 150 Hz).

A difference in the two resonant frequencies of about 5 mHz, obtained experimentally in the first prototype, and a difference in the two lengths of 0.5 mm, well within machining tolerances, provide us with a common mode rejection factor of about 6000. So, to reach the desired displacement sensitivity at 10 Hz, the suspension system must provide an additional factor of 2000 of vertical isolation at 10 Hz. This is achievable using

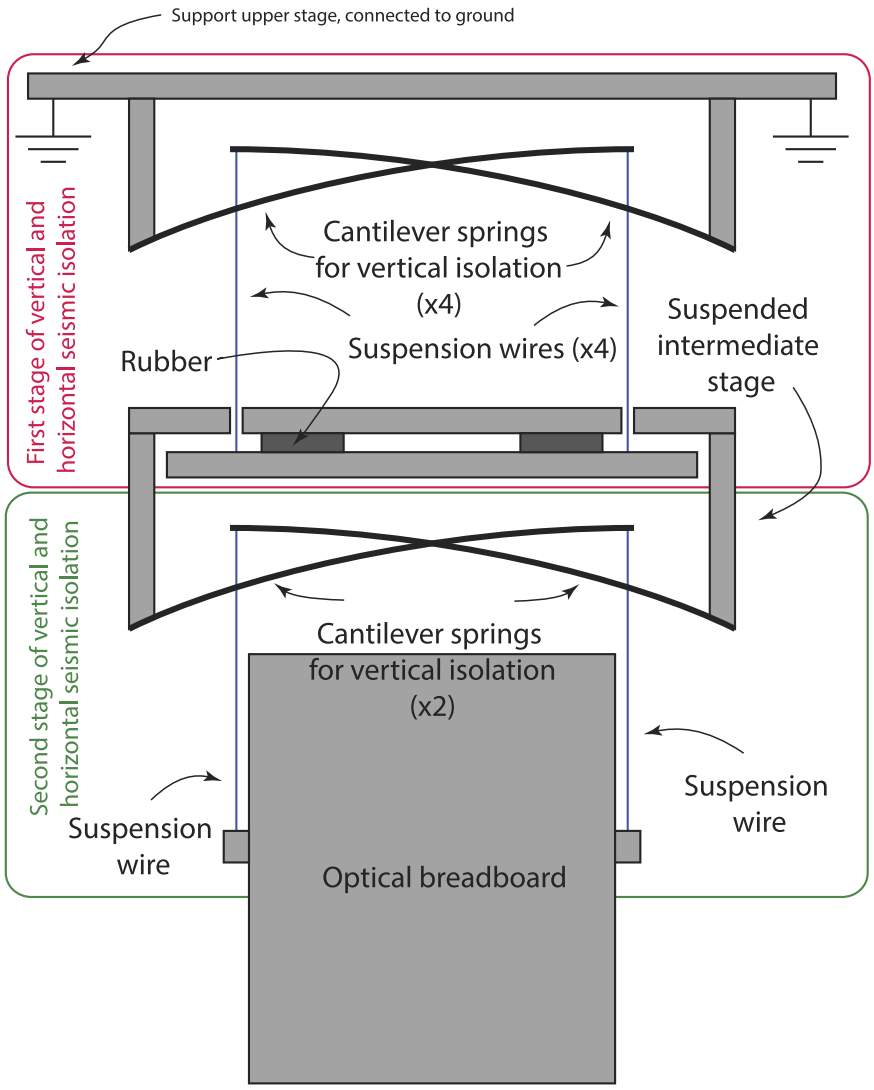

FIG. 7. A simplified schematic of the seismic isolation system, highlighting the key components and the two stages of vertical and horizontal isolation.

two cascaded stages with characteristic frequencies close to 2 Hz. Figure 7 shows a simplified schematic of the mechanical system. Each stage is composed of maraging steel cantilevers, roughly 30 cm long, 7 cm wide, and 2 mm thick. Four cantilevers suspend the intermediate stage from a support structure with steel wires, and two additional cantilevers support the optical breadboard from the intermediate stage, with another two wires attached to the sides of the board, above its center of mass. Each cantilever supports a load of about 10 kg, which corresponds to about 50% of their yield stress. Both the optical board and the intermediate stage have a mass of about 20 kg. The intermediate stage includes a stack of rubber to provide some passive damping of the suspension resonant modes.

D. Current sensitivity and noise sources

The design described in the Secs. IV A–IV C provides a theoretical sensitivity to displacement noise which is limited by shot noise at all frequencies above about 20 Hz at a level better than 10^{-15} m/$\sqrt{\text{Hz}}$. Figure 8 shows the measured sensitivity of the system in the present configuration. The same figure shows also the best sensitivity achieved with the first prototype of the experiment, as described in Sec. III. The vast improvement at low frequencies is very apparent. The additional traces in Fig. 8 show the projected contribution of various technical noises to the measured sensitivity. The sum of all those noise is capable of explaining almost all of the measured displacement noise. However, the contribution of seismic noise is much larger than what was foreseen in the design of the seismic isolation system, both at frequencies below 40 Hz and at frequencies above 200 Hz.

The main coupling path in the low frequency region has been identified as the following: since the optical board and the intermediate stage of the seismic isolation are suspended by multiple wires and cantilever springs, any difference in the stiffness of the springs causes a direct coupling of vertical motion of the suspension point to angular motion of the suspended body. In particular, the critical angular degree of freedom for our measurement is the roll motion of the optical board (i.e., rotation about an axis perpendicular to the board surface), since any motion in this degree of freedom will create a differential displacement of the two test cantilevers with

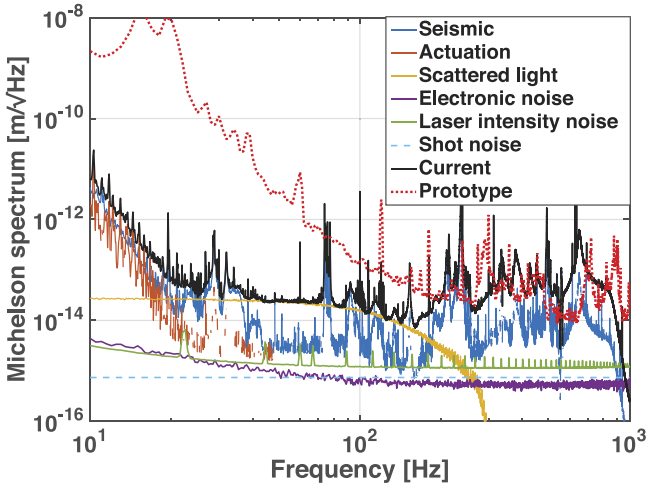

FIG. 8. Typical sensitivity of the measurement system in the present configuration (solid black trace) compared with the best obtained with the first prototype (dotted red line). The other traces show the contribution of various noise sources to the total displacement noise: actuation noise and scattered light noises are described in Sec. IV D; electronic noise refers to the sum of photodiode dark noise and analog-to-digital conversion noise; laser intensity noise and shot noise are discussed in Sec. II A.

respect to the Michelson beamsplitter. An imbalance of a few percent in the cantilever stiffnesses, well within manufacturing tolerances, is enough to explain this increased coupling of seismic noise at low frequency. We have designed a modification of the seismic isolation system, consisting of an additional stage to be added before the optical board, that will decouple vertical motion from angular motion. At higher frequencies, the increased coupling of seismic noise is also due to mismatched responses of the suspension cantilevers, this time in their internal resonant modes. This issue will also be mitigated by the addition of the angular decoupling stage as described above.

As discussed in Sec. II, the direct displacement sensitivity is not the ultimate limit to our measurement system, since the demodulation technique can detect periodic non-stationary noise below the sensing noise, provided that the latter is stationary. Therefore particular care is necessary for all sources of non-stationary noise, especially those that might be modulated by the common mode motion of the two cantilevers. Referring again to Fig. 8, two of the noise sources listed there are particularly problematic. Scattered light is intrinsically non-stationary, since the amplitude and maximum frequency of this noise source depend on the motion of the scattering element.[4] Scattered light has been mitigated with a careful placement of black glass absorbing baffles and beam dumps. All spurious beams from the anti-reflection coated surfaces are intercepted and dumped. This improvement will be sufficient to reduce scattered light below the target sensitivity. In addition the increased seismic isolation will also help in reducing scattered light. Indeed, scattered light up-conversion is highly non-linear:[4] residual motion at few Hz will be the dominant contributor to scattered light phase noise, while the slower 100 mHz motion that we will introduce to periodically stress the cantilevers results in a negligible contribution. The second potentially problematic non-stationary noise source can be traced to the actuation chain which used to apply force on the two test cantilevers. In particular, the digital-to-analog converters (DAC) are known to exhibit a significant amount of harmonic distortion. The low frequency common mode drive is up-converted in frequency by the DAC and results in a non-stationary noise at the level of the measured sensitivity. This issue is being tackled with an improvement of the control electronics.

Finally, Barkhausen noise in the magnets used for the vertical actuation of the test cantilevers can result in crackling noise like signals. To reduce the impact of Barkhausen noise, we are using SmCo magnets which have much lower noise than the more common NdFeB magnets.[22] The estimated contribution of this noise source is well below our present sensitivity.

V. DISCUSSION AND OUTLOOK

In this review, we presented an instrument designed for the study of the mechanical up-conversion phenomenon in metals. Two key points make the approach presented here different from previous studies. First of all, given the authors' involvement in the gravitational wave observatory Advanced LIGO, this system will study the behavior of metals in the elastic regime, far from the yield stress that would introduce plastic deformations. As already pointed out, to the best of our knowledge, there has been no experimental investigations of this kind in this regime. Second, since we expect the up-conversion events, if present, to be of very small amplitude, our intended measurement is not the detection of the single events, but rather the statistical properties of the up-conversion noise that arise as the incoherent sum of all the events. In particular, we are interested in the dependence of the noise power on the low frequency external disturbance the metal is subjected to.

At the time of writing, the experimental apparatus has been constructed and commissioned. Although it has not yet reached the design sensitivity, characterization of the background noise was successful. With a measured sensitivity level of a few 10^{-14} m/$\sqrt{\text{Hz}}$ at 50–100 Hz, the experiment has already reached a sensitivity level which is significantly better than the first prototype of the instrument. However, several limitations of the present setup have been already identified and are being tackled with small scale, short term modifications of the seismic isolation system and of the control electronics. We expect to reach a significantly improved sensitivity within a few months from the time of writing. This will allow meaningful upper limits to be set for the contribution of up-conversion noise to the Advanced LIGO detectors' sensitivities, and may possibly yield a direct detection of up-conversion noise in metals still operating within the elastic regime.

Clearly, one important point that has to be addressed is how to scale the results from the small test cantilevers used in our experiment to the much larger blades installed in the Advanced LIGO suspension. The derivation of this scaling is made more uncertain by the lack of a microscopical model of up-conversion noise in our regime. A discussion of those points is in the topic of another paper in preparation.

ACKNOWLEDGMENTS

We would like to thank the members from the Seismic Isolation and Suspension Working Group in the LIGO Scientific Collaboration for many enriching discussions. Also many thanks to Seiji Kawamura, Yuri Levin, and Rai Weiss for valuable contributions to the initial experiment, and to Federico Paoletti for help in the design of the electronics. LIGO was constructed by the California Institute of Technology and Massachusetts Institute of Technology with funding from the National Science Foundation, and operates under cooperative agreement PHY-0757058. Advanced LIGO was built under Award No. PHY-0823459. This paper carries LIGO Document No. LIGO-P1500272. This manuscript has an internal LIGO project designation of P1500272. J.R.G. gratefully acknowledges the financial support of NSF No. DMR-1204864.

[1]A. Yu. Ageev, I. A. Bilenko, and V. B. Braginsky, "Excess noise in the steel suspension wires for the laser gravitational wave detector," Phys. Lett. A **246**, 479 (1998).
[2]G. Cagnoli, L. Gammaitoni, J. Kovalik, F. Marchesoni, M. Punturo, S. Braccini, R. De Salvo, F. Fidecaro, and G. Losurdo, "Mechanical shot noise induced by creep in suspension devices," Phys. Lett. A **237**, 21 (1997).
[3]J. Aasi *et al.*, "Advanced LIGO," Classical Quantum Gravity **32**(7), 074001 (2015).
[4]T. Accadia *et al.*, "Noise from scattered light in virgo's second science run data," Classical Quantum Gravity **27**, 194011 (2010).
[5]S. M. Aston *et al.*, "Update on quadruple suspension design for advanced LIGO," Classical Quantum Gravity **29**, 235004 (2009).
[6]M. Beccaria *et al.*, "The creep problem in the virgo suspensions: A possible solution using maraging steel," Nucl. Instrum. Methods Phys. Res., Sect. A **404**, 455 (1998).
[7]J. Bechhoefer, "Feedback for physicists: A tutorial essay on control," Rev. Mod. Phys. **77**, 783 (2005).
[8]W. Blum, P. Eisenlohr, and F. Breutinger, "Understanding creep? A review," Metall. Mater. Trans. A **33**(2), 291 (2002).
[9]F. Bondu, P. Fritschel, C. N. Man, and A. Brillet, "Ultrahigh-spectral-purity laser for the virgo experiment," Opt. Lett. **21**, 582 (1996).
[10]S. Braccini *et al.*, "The maraging-steel blades of the virgo super attenuator," Meas. Sci. Technol. **11**, 467 (2000).
[11]S. Braccini *et al.*, "Monitoring the acoustic emission of the blades of the mirrors suspension for a gravitational wave interferometer," Phys. Lett. A **301**, 389 (2002).
[12]R. DeSalvo, A. DiCintio, and M. Lundin, "The role of self-organized criticality in elasticity of metallic springs: Observations of a new dissipation regime," Eur. Phys. J. Plus **126**, 1 (2011).
[13]G. Dieter, *Mechanical Metallurgy* (McGraw-Hill, 1986).
[14]D. M. Dimiduk, C. Woodward, R. LeSar, and M. D. Uchic, "Scale-free intermittent flow in crystal plasticity," Science **312**, 1188 (2006).
[15]N. Friedman *et al.*, "Statistics of dislocation slip avalanches in nanosized single crystals show tuned critical behavior predicted by a simple mean field model," Phys. Rev. Lett. **109**, 095507 (2012).
[16]G. D. Hammond, A. V. Cumming, J. Hough, R. Kumar, K. Tokmakov, S. Reid, and S. Rowan, "Reducing the suspension thermal noise of advanced gravitational wave detectors," Classical Quantum Gravity **29**(12), 124009 (2012).
[17]R. Maass, M. Wraith, J. T. Uhl, J. R. Greer, and K. A. Dahmen, "Slip statistics of dislocation avalanches under different loading modes," Phys. Rev. E **91**, 042403 (2015).
[18]F. Matichard *et al.*, "Seismic isolation of advanced LIGO: Review of strategy, instrumentation and performance," Classical Quantum Gravity **32**, 185003 (2015).
[19]A. Michelson and E. Morley, "On the relative motion of the earth and the luminiferous ether," Am. J. Sci. **34**, 333 (1887).
[20]J. Sethna, K. Dahmen, and C. R. Myers, "Crackling noise," Nature **410**, 242 (2001).
[21]G. Vajente, E. A. Quintero, and X. Ni, "Upper limits on crackling noise from the crackle1 apparatus," LIGO Document T1400752, 2014.
[22]R. Weiss and D. Kelley, "Collection of reports on Barkhausen noise," LIGO Document T0900061, 2009.